IEEE Access
Multidisciplinary | Rapid Review | Open Access Journal

Received July 8, 2019, accepted July 23, 2019, date of publication July 25, 2019, date of current version August 8, 2019.

Digital Object Identifier 10.1109/ACCESS.2019.2931141

A Balanced Filtering Quasi-Yagi Antenna With Low Cross-Polarization Levels and High Common-Mode Suppression

FENG WEI, (Member, IEEE), XI-BEI ZHAO, (Student Member, IEEE), AND XIAO WEI SHI, (Senior Member, IEEE)

Key Laboratory of Antennas and Microwave Technology, School of Electronic Engineering, Xidian University, Xi'an 10701, China

Corresponding author: Xi-Bei Zhao (xibeiz@stu.xidian.edu.cn)

This work was supported in part by the Fundamental Research Funds for the Central Universities under Grant JB180204, in part by the State Key Laboratory of Metamaterial Electromagnetic Modulation Technology under Grant GYL08-1444, and in part by the Innovation Fund of Xidian University.

ABSTRACT A balanced planar quasi-Yagi antenna integrated with a bandpass filtering response is presented in this paper. The proposed balanced antenna consists of a balanced stepped-impedance microstrip-slotline transition structure, a driver dipole, a parasitic strip, and a bandpass filtering unit. A good differential-mode (DM) passband selectivity is formed by inserting a microstrip stub-loaded resonator (SLR) in the feed line of the quasi-Yagi antenna. This integration enables the antenna to achieve both compact size and high frequency selectivity. By controlling the dimensions of SLR, the central frequency and fractional bandwidth (FBW) can be easy to be adjusted. Meanwhile, the microstrip-slotline transition structure can achieve a good wideband common-mode (CM) suppression without affecting the DM ones, thus simplify the design procedure. The proposed antenna with low cross-polarization level and high CM rejection is found to be comparable to the conventional quasi-Yagi antenna. Furthermore, there are two radiation nulls on both sides of the passband to improve the selectivity effectively. In order to validate its practicability, the balanced antenna is designed and fabricated. The experimental results exhibit that the designed balanced filtering antenna features good filtering response, low cross-polarization level, and high CM rejection.

INDEX TERMS Balanced antenna, filtering antenna, CM suppression, low cross-polarization.

I. INTRODUCTION

In recent years, balanced circuits have attracted great attention and have been more and more utilized because of the high immunity to the environmental noise, interference and crosstalk between different elements, compared with the single ended counterparts. In order to build up fully balanced transceivers, balanced antennas and components are adopted for differential signals operation due to the direct integration with differential circuits. Recently, some balanced components and antennas were designed [1]–[4]. Microstrip to slotline transition structure are widely used in the design of balanced filters with intrinsic common-mode suppression. The balanced filter utilizing such structure were first designed in 2012 [5]. Some succeeding work to enhance the selectivity and control the bandwidth were also proposed [6]–[8].On the other hand, integrated design of circuit components for realizing miniaturization and improved performance has become a trend. Filters and antennas, due to their importance in wireless communication systems, have been often integrated into a single module in circuit design, which is referred to as filtering antennas [9]–[14]. In [12], a wideband quasi-Yagi antenna, fed by a balun bandpass filter, was designed with a compact size. In [13], a low-profile planar filtering dipole antenna was presented with high out-of-band radiation rejection levels by generating three radiation nulls. In [14], a compact antenna as the last resonator of the filter was proposed to reduce the overall size with high band-edge gain selectivity. Although these filtering antennas obtain good filtering response, they are single-end type. In [15], a balanced filtering antenna was realized by inserting a double-sided parallel-strip line filter between the driver and the reflector of the quasi-Yagi antenna. In [16], a balanced microstrip antenna array with third-order Chebyshev filtering response

The associate editor coordinating the review of this manuscript and approving it for publication was Yingsong Li.

fed by two resonators was designed. However, there is no radiation nulls in above designs. Therefore, developing high-performance balanced filtering antennas still is a challenging task.

In this paper, a balanced planar quasi-Yagi antenna integrated with a bandpass filtering response is analyzed and designed. The designed antenna is fed by a balanced U-type microstrip-slotline transition structure, which can realize an independent common-mode (CM) response with a broader bandwidth and a better suppression. Since all the CM signals are intrinsically blocked, only its differential-mode (DM) passband performance needs to be investigated in the design, which simplifies the design procedure significantly. Meanwhile, a stub-loaded resonator (SLR) is employed to realize a steep passband with an adjustable fractional bandwidth (FBW). Meanwhile, the proposed balanced filtering antenna achieves high frequency selectivity and low cross-polarization levels without increasing the overall size. In order to validate the design strategies, a balanced filtering antenna convering from 3.59 to 4.32 GHz was fabricated and a good agreement between the simulated and measured results is observed. In addition, the maximum cross-polarization levels are less than −24dB within the DM passband.

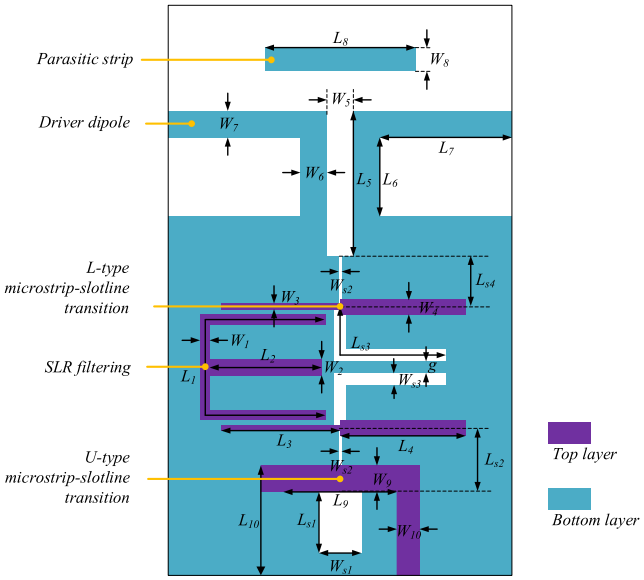

FIGURE 1. Configuration of the proposed balanced filtering antenna.

II. ANALYSIS AND DESIGN OF BALANCED FILTERING ANTENNA

A. OVERALL STRUCTURE AND DESIGN PRINCIPLE

Fig. 1 shows the configuration and parameters of the proposed planar balanced filtering quasi-Yagi antenna. The designed antenna is printed on a F4BM substrate with a dielectric constant of 2.2 and a thickness of 0.8 mm. It consists of a balanced U-type microstrip-slotline transition structure as the feed line, a pair of L-type microstrip-slotline transition structures, a microstrip SLR as the filtering element, one driver dipole as the main radiation unit and one parasitic strip as the director. The driver dipole and the parasitic strip are printed on the bottom layer of the substrate, whereas the microstrip feeding line and SLR are printed on the top layer of the substrate. The slotline on the ground plane of a substrate is crossed at a right angle with the U-type microstrip line on its opposite interface. Meanwhile, the slotline resonator extends about a quarter of wavelength beyond the U-type microstrip line. In order to obtain a miniaturization, a stepped-impedance slotline is adopted, which is similar to the stepped-impedance resonator (SIR). Further, a pair of symmetrical L-type microstrip-slotline transition structures and an SLR are employed to achieve a good bandpass response. The driver dipole is connected to the ground plane through a slotline. The length of the driver dipole is equal to the width of the ground plane. The signals transmission is summarized as follows: Firstly, the input signals are fed into the balanced U-type microstrip transition on top layer. Through strong magnetic coupling, the DM signals along the U-type microstrip line can be converted successfully into the slotline mode propagating along the slotline on bottom layer. Secondly, the signals in the slotline are coupled with the top layer microstrip line of the L-type slotline to microstrip transition structure. Thirdly, through the parallel coupling, the signals are transferred into the microstrip bandpass response structure. Then, the signals after filtering are transferred to the antenna through the L-type microstrip to slotline transition structure. This transformation process is antithetical with the second step. Finally, the antenna radiates the signals with a good DM passband selectivity.

B. ANALYSIS OF BANDPASS RESPONSE

The conventional SLR comprises a common microstrip half-wavelength resonator and an open stub loaded at the center, as shown in Fig. 2, where Y_1, L_1, Y_2 and L_2 denote the characteristic admittances and lengths of the microstrip line and open stub, respectively. Because of the geometrical symmetry, odd- and even-mode analysis can be adopted to characterize it [4].

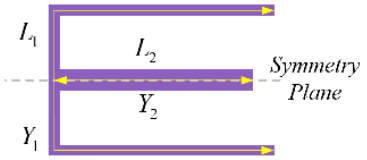

FIGURE 2. Configuration of SLR.

For even-mode, there is an equivalent symmetric magnetic wall. Then, the structure can be bisected with open circuit at its middle part, and the equivalent circuit is shown in Fig. 3. For the special case of $Y_2 = 2Y_1$, the even-mode resonant frequencies can be deduced as:

$$f_{even} = \frac{nc}{(L_1 + 2L_2)\sqrt{\varepsilon_{eff}}} \tag{1}$$

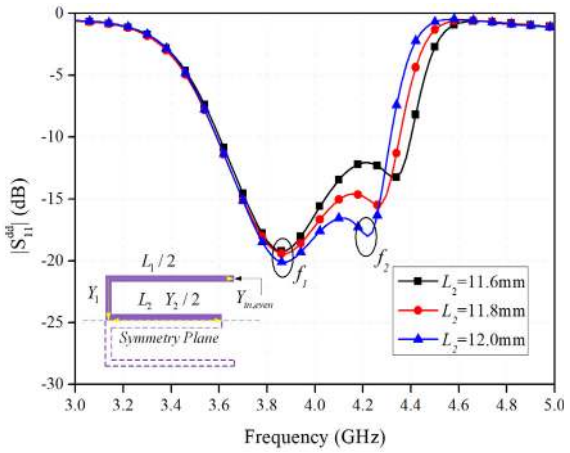

FIGURE 3. Simulated reflection coefficients of the proposed antenna for various L_2.

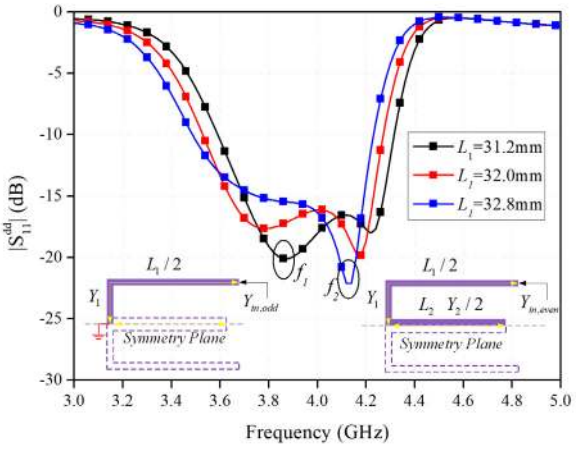

FIGURE 4. Simulated reflection coefficients of the proposed antenna for various L_1.

where n is a natural number, c is the speed of the light in free space, and ε_{eff} stands for the effective dielectric constant of the substrate. When $n = 1$, the fundamental resonant frequency can be obtained as:

$$f_2 = f_{even} = \frac{c}{(L_1 + 2L_2)\sqrt{\varepsilon_{eff}}} \tag{2}$$

Fig. 3 gives the effects of the parameter L_2 on the DM reflection coefficient. When the length $L_1 = 31.2$ mm (corresponding to $\lambda_g/2$ at the fundamental odd-mode resonant frequency f_1), by changing the open stub length L_2, f_2 can be shifted accordingly, whereas f_1 is maintained unchanged. It can be observed that only f_2 moves toward the higher frequency band as L_2 decreases. The reason for this is that decreasing the physical size of the open-stub will affect only f_{even}.

Under the odd-mode excitation, there is an equivalent symmetric electric wall, which leads to the equivalent circuit as shown in Fig. 4. Therefore, the odd-mode resonant frequencies can be derived as:

$$f_{odd} = \frac{(2n-1)c}{2L_1\sqrt{\varepsilon_{eff}}} \tag{3}$$

When $n = 1$, the fundamental resonant frequency can be written as:

$$f_1 = f_{odd} = \frac{c}{2L_1\sqrt{\varepsilon_{eff}}} \tag{4}$$

Fig. 4 gives the effects of the parameter L_1 on the DM reflection coefficient. When the length $L_2 = 12$ mm, it can be observed that the resonant frequencies will decrease as L_1 increases. The reason for this is that increasing the physical size of a half wavelength microstrip resonator will affect the fundamental odd-mode resonant frequency f_1 and the fundamental even-mode resonant frequency f_2 accordingly. Meanwhile, it can also be observed that the odd-mode resonant frequency is not affected by the open stub.

With the above analysis, it can be noted that by properly controlling the dimensions of the SLR structure, an adjustable DM bandwidth can be realized. Therefore, both the center frequency and FBW of the designed filtering antenna are easy to be controlled. And the CM responses remain almost unchanged with these two parameters, which are not given here due to the length of the paper.

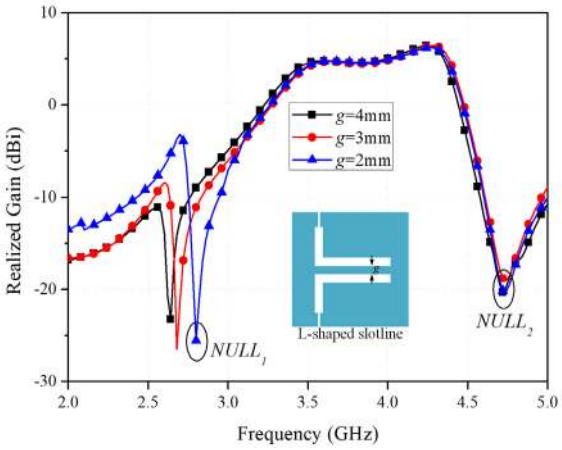

FIGURE 5. Positions change of $NULL_1$ with different g.

In addition, there are two radiation nulls ($NULL_1$ and $NULL_2$) be engendered on the both sides of the passband to improve the selectivity effectively, as illustrated in Fig. 5. $NULL_1$ can be generated and individually controlled by changing of the cross coupling between the L-type slotlines. However, the input signals can also be transferred into the driver dipole through the coupling of the two L-type slotlines. The distance between slotlines is closer, the coupling is stronger, and the gain produced by this way is enhancer. It can be observed that $NULL_1$ moves toward the lower frequency as g increases, whereas $NULL_2$ is maintained unchanged. $NULL_2$ is generated because of the intrinsic performances of the embedded SLR. Meanwhile the location of $NULL_2$

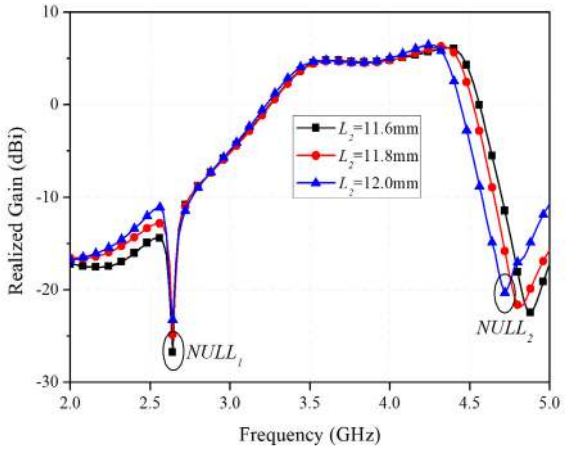

FIGURE 6. Positions change of $NULL_2$ with different dimensions of L_2.

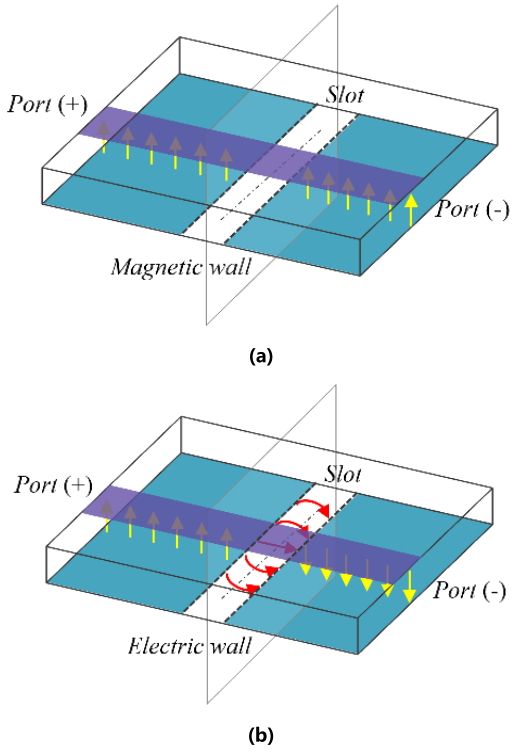

FIGURE 7. Electrical field distribution of the balanced microstrip-slotline transition structure. (a) Under CM operation. (b) Under DM operation.

has a direct correlation with the length of the open stub L_2, illustrated in Fig. 6. When the length of L_2 changes from 11.6mm to 12mm, the position of $NULL_2$ moves to the lower frequencies, whereas the position of $NULL_1$ is maintained unchanged. Therefore, the selectivity of the balanced antenna can be greatly enhanced and controlled by generating $NULL_1$ and $NULL_2$.

C. BALANCED MICROSTRIP/SLOTLINE TRANSITION STRUCTURE

To analyze the principle of CM suppression, Fig. 7 depicts the electrical field distribution of the balanced feeding

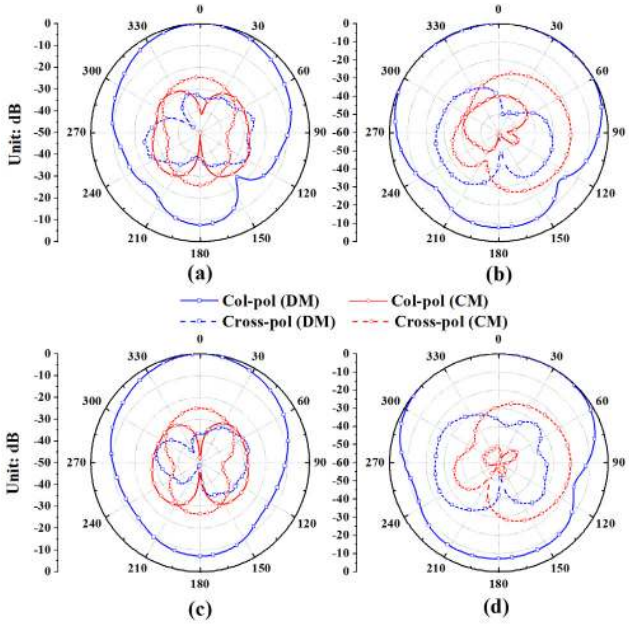

FIGURE 8. Radiation patterns of the proposed balanced antenna under DM and CM operation at (a) 3.77 GHz (E-plane), (b) 3.77 GHz (H-plane), and (c) 4.16 GHz (E-plane), (d) 4.16 GHz (H-plane).

line structure. The designed balanced antenna is fed by a balanced microstrip-slotline transition structure, which is composed of a U-type microstrip feedline and a slotline. Further, stepped-impedance microstrip line and slotline are employed to obtain a better impedance matching and miniaturization. It is important to underline that such structure serves a great CM suppression. Under CM excitation, the two feeding ports of the proposed antenna are excited by the signals with the same amplitudes and phases, as shown in Fig. 7 (a). A virtual magnetic wall is generated that the CM signals will offset each other on the slotline. Therefore, there is nearly no any vertical electrical field flowing through the slot, which means that only small energy can be coupled to SLR. Thus, high CM suppression is realized. On the other hand, for a DM operation, the DM signals along the microstrip lines can be transmitted to SLR through strong magnetic coupling, and thus, the input DM signals can be effectively radiated. As is shown in Fig. 7(b), the balanced stepped-impedance microstrip-slotline transition structure can transmit DM signals to the next transition along the slotline through the virtual electric wall by the strong coupling between the microstrip line and slotline. Meanwhile, the DM design is independent from the CM one according to the analysis above because the CM signals can hardly pass through the mircostrip-slotline transition structures. Thus, the design procedure can be greatly simplified. For further illustrate the CM suppression of the designed antenna, Fig. 8 shows the simulated gain radiation patterns of the proposed antenna under CM and DM operation at 3.77 and 4.16GHz, respectively. It can be seen that the simulated CM peak gains of the maximum copolarization in E- and H-planes are −25.8 and −33.2 dBi, and the maximum cross-polarization in E- and H-planes are

−24.6 and −20.5 dBi, respectively. Therefore, there is almost no CM signals which transfer into the driver dipole of the proposed antenna. It indicates that the CM radiation is effectively suppressed by introducing the balanced microstrip-slotline transition structure, while the DM radiation pattern remains stable in the passband.

D. DESIGN GUIDELINE

Based on the above analysis and discussions, a simple design procedure of the proposed balanced filtering quasi-Yagi antenna can be summarized as follows.

1) The U-type microstrip-slotline transition structure: Realizable electrical lengths and characteristic impedances of microstrip lines and slotlines can be chosen according to our previous works in [4].

2) The L-type slotline-microstrip transition structure: Design the L-type slotline-microstrip transition structure is inserted between the DM feeding structure in 1) and the microstrip filtering in 3).

3) The microstrip SLR structure: For the desired center frequency and filter bandwidth, the physical widths and lengths of every line sections of the SLR can be selected appropriately according to (3), and (4).

4) The quasi-Yagi antenna: Design the quasi-Yagi antenna according to the traditional quasi-Yagi antenna design method, consist of the radiating driver dipole which connected the slotline through coplanar stripline, and the parasitic strip on the bottom layer.

5) Optimization and Fabrication: Further optimize all values to realize better DM and CM responses and radiation performance of the proposed antenna. Full-wave electromagnetic simulation and dimension optimization in the commercial simulation software HFSS can be conducted.

III. SIMULATION AND MEASUREMENT RESULTS

The balanced filtering quasi-Yagi antenna is fabricated with its photo shown in Fig.9. The detailed dimensions of the proposed antenna are listed in Table 1.

The measured S-parameters, which are measured with an Agilent VNA (vector network analyzer) N5230A, and peak antenna gains of the antenna prototype are compared with the simulation ones in Fig. 10. It can be seen that the measured results agree well with the simulated ones over the entire operation frequency range. For DM response, the measured two resonant frequencies are at 3.76 GHz and 4.15 GHz, which are very close to the simulated ones (3.77 GHz & 4.16 GHz). The DM impedance bandwidth for |Sdd 11| < −10 dB is 18.5% (3.59 to 4.32 GHz). For CM response, it can be observed that the simulated and measured |Scc 11| of the proposed balanced antenna is larger than −0.32 dB within the operating bands, which means that almost all CM signals are return back to the input ports. Therefore, a high level of CM suppression is obtained. For radiation gain, the measured DM broadside antenna gains are 4.17 dBi and 5.82 dBi at 3.77 GHz and 4.16GHz, while the simulated ones are 4.65 dBi and 6.06 dBi, respectively. Meanwhile, two

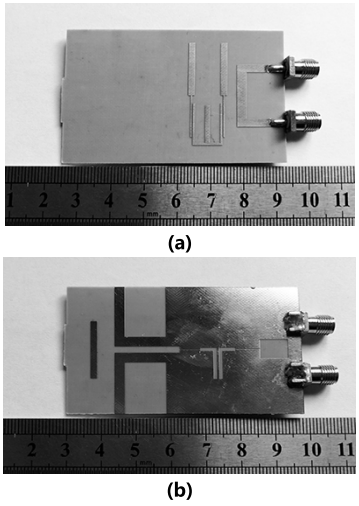

FIGURE 9. Photographs of the proposed balanced antenna. (a) Front object. (b) Back object.

TABLE 1. Dimensions of the proposed balanced filtering antenna.

Parameters	W_1	W_2	W_3	W_4	W_5	W_6	W_7
Value/mm	0.7	1.5	0.5	1.2	2	3	3
Parameters	W_8	W_9	W_{10}	W_{s1}	W_{s2}	W_{s3}	L_1
Value/mm	2	3	2.4	8	0.2	1	31.2
Parameters	L_2	L_3	L_4	L_5	L_6	L_7	L_8
Value/mm	12	12.5	16	19	12	16	18
Parameters	L_9	L_{10}	L_{s1}	L_{s2}	L_{s3}	L_{s4}	g
Value/mm	14	15	10	7	13.5	6	4

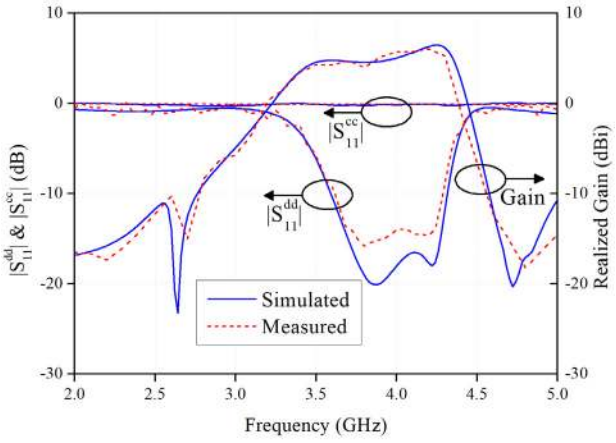

FIGURE 10. Simulated and measured S-parameters and realized broadside antenna gain.

radiation nulls at 2.63 GHz and 4.72 GHz are generated, which are located at the both sides of the DM passband, respectively. The in-band gain responses are all not so flat that is because of the variation gain of the broadband quasi-Yagi antennas itself as shown in [18], [19]. The deviations of the measurements from the simulations are expected mainly due to the reflections from the connectors and the finite substrate.

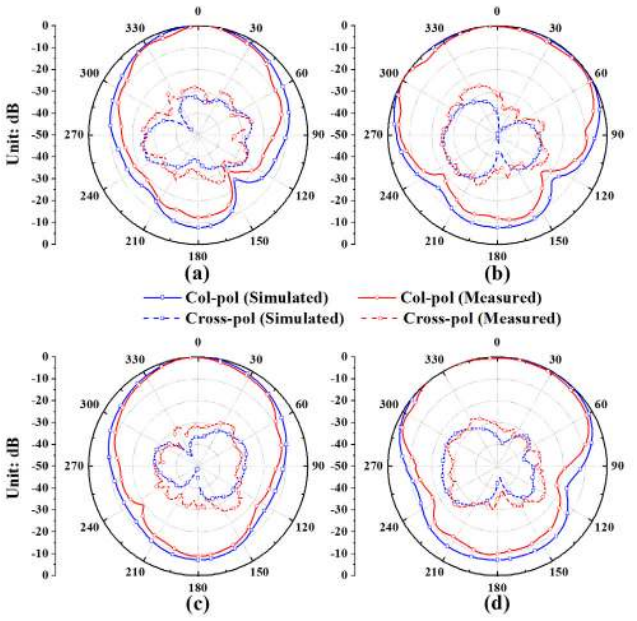

FIGURE 11. Comparisons of the Simulated and measured radiation patterns of the antenna under DM operation at (a) 3.77 GHz (E-plane), (b) 3.77 GHz (H-plane), and (c) 4.16 GHz (E-plane), (d) 4.16 GHz (H-plane).

TABLE 2. Comparison with some reported filtering antenna.

Ref.	f_0 (GHz)	Differential input	Radiation nulls	XPOL (dB)	CM suppression (dB)
[13]	4.5	No	3	~ -20	-
[14]	2.45	No	2	-10	-
[15]	1.82	Yes	0	-17	-
[17]	5.39	Yes	0	~ -20	2.37
This work	**3.96**	**Yes**	**2**	**-24**	**0.32**

Fig. 11 compares the simulated and measured radiation patterns of the balanced filtering antenna under DM operation. A balun with 180° phase difference is utilized to provide the DM signals for the measurement. It can be observed that the radiation pattern remains stable within the operating band. The simulated and measured maximum gains of the cross-polarization radiations in E- and H-planes are −24.8 and −25.2 dB, respectively, which show that low cross-polarization levels of DM response are obtained for the balanced filtering antenna.

A comparison of the performance of the proposed filtering antenna with other reported ones is listed in Table 2. The proposed antenna features steep filtering response, low cross-polarization levels and high CM rejection. The simpler structure and better performance make the proposed antenna competitive and promising for the balanced wireless communications system.

IV. CONCLUSION

This paper has proposed a balanced filtering antenna with superior filtering response, a high CM suppression and a low cross-polarization. Owing to the adopted balanced stepped-impedance microstrip-slotline transition structure, the CM suppression is improved and the low cross-polarization is obtained. Meanwhile, SLR is applied to introduce two radiation nulls outside the passband and realize great flexibility to adjust the DM bandwidth. The measured cross-polarization level is −24 dB and the measured CM reflection coefficient is larger than −0.32 dB within the operating band. The proposed balanced filtering antenna is attractive for the balanced wireless communication systems.

REFERENCES

[1] Y.-Y. Liu and Z.-H. Tu, "Compact differential band-notched stepped-slot UWB-MIMO antenna with common-mode suppression," *IEEE Antennas Wireless Propag. Lett.*, vol. 16, pp. 593–596, 2017.

[2] F. Wei, X. T. Zou, X. Y. Wang, B. Li, and X. B. Zhao, "A differential UWB quasi-yagi antenna with a reconfigurable notched band," *Frequenz*, vol. 72, nos. 9–10, pp. 401–406, Sep. 2018.

[3] C.-H. Lee, J.-H. Wu, C.-I. G. Hsu, H.-L. Chan, and H.-H. Chen, "Balanced band-notched UWB filtering circular patch antenna with common-mode suppression," *IEEE Antennas Wireless Propag. Lett.*, vol. 16, pp. 2812–2815, 2017.

[4] F. Wei, Z.-J. Yang, P.-Y. Qin, Y. Jay Guo, B. Li, and X.-W. Shi, "A balanced-to-balanced in-phase filtering power divider with high selectivity and isolation," *IEEE Trans. Microw. Theory Techn.*, vol. 67, no. 2, pp. 683–694, Feb. 2019.

[5] Y.-J. Lu, S.-Y. Chen, and P. Hsu, "A differential-mode wideband bandpass filter with enhanced common-mode suppression using slotline resonator," *IEEE Microw. Wireless Compon. Lett.*, vol. 22, no. 10, pp. 503–505, Oct. 2012.

[6] D. Chen, H. Bu, L. Zhu, and C. Cheng, "A differential-mode wideband bandpass filter on slotline multi-mode resonator with controllable bandwidth," *IEEE Microw. Wireless Compon. Lett.*, vol. 25, no. 1, pp. 28–30, Jan. 2015.

[7] X. Guo, L. Zhu, and W. Wu, "Strip-loaded slotline resonators for differential wideband bandpass filters with intrinsic common-mode rejection," *IEEE Trans. Microw. Theory Techn.*, vol. 64, no. 2, pp. 450–458, Feb. 2016.

[8] W. Feng and W. Che, "Novel wideband differential bandpass filters based on T-shaped structure," *IEEE Trans. Microw. Theory Techn.*, vol. 60, no. 6, pp. 1560–1568, Jun. 2012.

[9] Y. Yusuf, H. Cheng, and X. Gong, "A seamless integration of 3-D vertical filters with highly efficient slot antennas," *IEEE Trans. Antennas Propag.*, vol. 59, no. 11, pp. 4016–4022, Nov. 2011.

[10] T.-L. Wu, Y.-M. Pan, P.-F. Hu, and S.-Y. Zheng, "Design of a low profile and compact omnidirectional filtering patch antenna," *IEEE Access*, vol. 5, pp. 1082–1089, 2017.

[11] J. Deng, S. Hou, L. Zhao, and L. Guo, "A reconfigurable filtering antenna with integrated bandpass filters for UWB/WLAN applications," *IEEE Trans. Antennas Propag.*, vol. 66, no. 1, pp. 401–404, Jan. 2018.

[12] C.-H. Wu, C.-H. Wang, S.-Y. Chen, and C. H. Chen, "Balanced-to-unbalanced bandpass filters and the antenna application," *IEEE Trans. Microw. Theory Techn.*, vol. 56, no. 11, pp. 2474–2482, Nov. 2008.

[13] Y. Zhang, X. Y. Zhang, and Y. M. Pan, "Low-profile planar filtering dipole antenna with omnidirectional radiation pattern," *IEEE Trans. Antennas Propag.*, vol. 66, no. 3, pp. 1124–1132, Mar. 2018.

[14] C.-T. Chuang and S.-J. Chung, "A compact printed filtering antenna using a ground-intruded coupled line resonator," *IEEE Trans. Antennas Propag.*, vol. 59, no. 10, pp. 3630–3637, Oct. 2011.

[15] J. Shi, X. Wu, Z. N. Chen, X. Qing, L. Lin, J. Chen, and Z.-H. Bao, "A compact differential filtering quasi-Yagi antenna with high frequency selectivity and low cross-polarization levels," *IEEE Antennas Wireless Propag. Lett.*, vol. 14, pp. 1573–1576, 2015.

[16] H.-T. Hu, F.-C. Chen, J.-F. Qian, and Q.-X. Chu, "A differential filtering microstrip antenna array with intrinsic common-mode rejection," *IEEE Trans. Antennas Propag.*, vol. 65, no. 12, pp. 7361–7365, Dec. 2017.

[17] C.-H. Lee, H.-H. Chen, W.-T. Shih, and C.-I. G. Hsu, "Balanced wideband filtering planar inverted-F antenna design," *IEEE Antennas Wireless Propag. Lett.*, vol. 16, pp. 716–719, 2017.

[18] J. Wu, Z. Zhao, Z. Nie, and Q.-H. Liu, "Bandwidth enhancement of a planar printed Quasi-Yagi antenna with size reduction," *IEEE Trans. Antennas Propag.*, vol. 62, no. 1, pp. 463–467, Jan. 2014.
[19] A. Abbosh, "Ultra-wideband quasi-Yagi antenna using dual-resonant driver and integrated balun of stepped impedance coupled structure," *IEEE Trans. Antennas Propag.*, vol. 61, no. 7, pp. 3885–3888, Jul. 2013.

FENG WEI was born in Shaanxi, China, in 1978. He received the B.Eng. and M.Eng. degrees in electrical engineering from Xidian University, Xi'an, China, in 2001 and 2004, respectively, and the Ph.D. degree in electrical engineering from Xidian University, in 2009. From 2004 to 2006, he was an RF Engineer with ZTE Corporation. Since 2009, he has been with the Collaborative Innovation Center of Information Sensing and Understanding, Xidian University, and the National Key Laboratory of Antennas and Microwave Technology, Xidian University, as a Lecturer, and an Associate Professor. From 2013 to 2014, he was a Visiting Scholar with the Commonwealth Scientific and Industrial Research Organization (CSIRO), Australia. He has authored or coauthored over 60 international and regional refereed journal papers. His recent research interests are mainly in the design of microwave components, circuits, and RFID system. He is a Senior Member of the CIE. He has served as a Reviewer for the IEEE TRANSACTIONS ON MICROWAVE THEORY AND TECHNIQUES and the IEEE MICROWAVE AND WIRELESS COMPONENTS LETTERS.

XI-BEI ZHAO was born in Heilongjiang, China, in 1995. She received the B.Eng. degree from the School of Electronic Engineering, Xidian University, Xi'an, China, in 2017, where she is currently pursuing the master's degree in antenna and microwave.

XIAO WEI SHI received the B.Sc. degree in radio physics, and the M.Eng. and Ph.D. degrees in electrical engineering from Xidian University, Xi'an, China, in 1982, 1990, and 1995, respectively. Since 1990, he has been with the National Key Laboratory of Antennas and Microwave Technology, Xidian University, as a Lecturer, an Associate Professor, and a Professor. He is also the Director of the Office for Science and Technology, Xidian University. He worked as a Postdoctoral Fellow with the Electronics and Telecommunications Research Institute (ETRI), South Korea, from 1996 to 1997. He has published over 50 international and regional refereed journal papers. His recent research interests are mainly in smart antennas design, electromagnetic inverse scattering, and electromagnetic compatibility. He received the First-Class Prize of Excellent Teaching of Shaanxi Province, in 1995, and the Scientific Progress Awards of Shaanxi Province, in 1992.